Engineering two-dimensional nonlinear photonic quasi-crystals

Alon Bahabad,* Ayelet Ganany-Padowicz, and Ady Arie

Department of Physical Electronics, Fleischman Faculty of Engineering, Tel-Aviv University, Tel Aviv 69978, Israel
**Corresponding author: alonuria@gmail.com*

Received January 17, 2008; revised April 15, 2008; accepted April 15, 2008;
posted May 21, 2008 (Doc. ID 91511); published June 13, 2008

A known algorithm for modeling quasi-periodic lattices is used to generate two-dimensional quadratic nonlinear photonic quasi-crystals containing a set of desired discrete spectral components. This allows us to fabricate optical devices in which an arbitrary set of nonlinear optical processes can be efficient. We demonstrate this capability by fabricating two devices: a multidirectional single-frequency doubler and a multidirectional, multifrequency doubler that is capable of nearly collinear doubling of cw radiation in the optical communication C band (1530–1570 nm) through angle tuning. © 2008 Optical Society of America

OCIS codes: 190.0190, 190.2620, 190.4223.

Often, a nonlinear optical process involving more than one frequency is inefficient, owing to material dispersion, causing the interacting beams to propagate with different velocities and so be out of phase with each other (phase mismatch). A flexible remedy known as quasi-phase matching (QPM) [1], uses spatial modulation of the relevant component of the nonlinear susceptibility tensor. To phase match several processes, as required, for example, for multiharmonic generation [2] or for specific schemes of all-optical switching [3], the spatial modulation should contain significant Fourier components at frequencies equal to the different phase-mismatch values. Several types of modulations, able to efficiently phase match a few processes (typically three or less) were suggested [2,4–11]; all of them are discrete in nature, and their spectrum is spanned by a finite number of primitive reciprocal lattice vectors (RLVs). Among those, two-dimensional quasi-periodic structures are especially interesting, owing to their extremely rich spectral content and optional high rotational symmetries [9–11]. However, no real procedure to engineer their RLV-based optical properties was used. Here, we use a recent solution to the general problem of phase matching an arbitrary set of nonlinear optical processes [12–14] to engineer two-dimensional nonlinear photonic quasi-crystals (NPQCs) with arbitrary spectral content. Two such NPQCs are experimentally demonstrated. One is the SHG fan, where three of its RLVs are predetermined to efficiently phase match collinear second-harmonic-generation (SHG) of 1550 nm at three propagation directions: $0°, \pm 20°$. The other is the frequency fan, where five of its RLVs are predetermined to efficiently phase match collinear SHG of the wavelengths 1530, 1540, 1550, 1560, and 1570 nm at propagation directions of −25°, −12.5°, 0°, 12.5°, and 25°, respectively. Using these RLVs and angle tuning it is possible to (nearly) double collinearly the entire communication C band (1530–1570 nm).

Both NPQCs were fabricated using electric-field poling of stoichiometric $LiTaO_3$. For a chosen operating temperature of 100 °C, the phase-mismatch magnitudes for all three processes of the SHG fan were calculated to be [15] $0.3012\ \mu m^{-1}$, whereas those of the frequency fan were 0.3093, 0.3052, 0.3012, 0.2973, and $0.2935\ \mu m^{-1}$ (starting with the 1530 nm SHG process). The spectrum of the NPQCs should contain these values as RLVs oriented at the angles indicated above. The solution we use [12] to realize the nonlinear photonic quasi-crystals is an adaption of the dual-grid method, originally used to create geometric models of quasi-crystals. The key property of this method is its ability to generate structures with an arbitrary predefined discrete spectral content. With the dual-grid method, we can get the tiling vectors spanning the quasi-crystal through an orthogonality relation in a "number of required processes"-dimensional space (three-dimensional and five-dimensional for the present cases). The tiling vectors of the SHG fan are found to be $7.54\ \mu m \angle 0°$, $31.31\ \mu m \angle 76.9°$, and $31.31\ \mu m \angle -76.9°$. Those of the frequency fan are $20\ \mu m \angle -78.3°$, $10.6\ \mu m \angle -65.3°$, $4.6\ \mu m \angle 6.5°$, $11.3\ \mu m \angle 66.4°$, and $20\ \mu m \angle 77.7°$. The quasi-periodic lattices defining each NPQC are made of parallelogram tiles whose number is equal to the possible number of ways to choose a pair of tiling vectors: $C_3^2=3$ for the SHG fan and $C_5^2=10$ for the frequency fan. The dual-grid method gives us the topology of the lattice–how the different tiles fit together. The lattice of both devices can be seen in Fig. 1, embedded upon a microscope image of a small part of the NPQC. To generate the NPQC pattern, every tile of the lattice is associated with a physical building block. For easy fabrication we chose circular motifs centered at the parallelogram's diagonal bisection points, in which the nonlinear tensor component of the polarization is given at a positive value: $+\chi^{(2)}$. The background is made with negative polarization $-\chi^{(2)}$. We used a numerical optimization procedure to find the best motifs radii for each tile, which provides the best frequency-doubling efficiencies for the desired processes [7]. The best results for each device were given for the maximal circle motif within the largest of the parallelograms (a 6.9 μm radius for the SHG fan and a 4 μm radius for the frequency fan) and no circle motifs at all

0146-9592/08/121386-3/$15.00

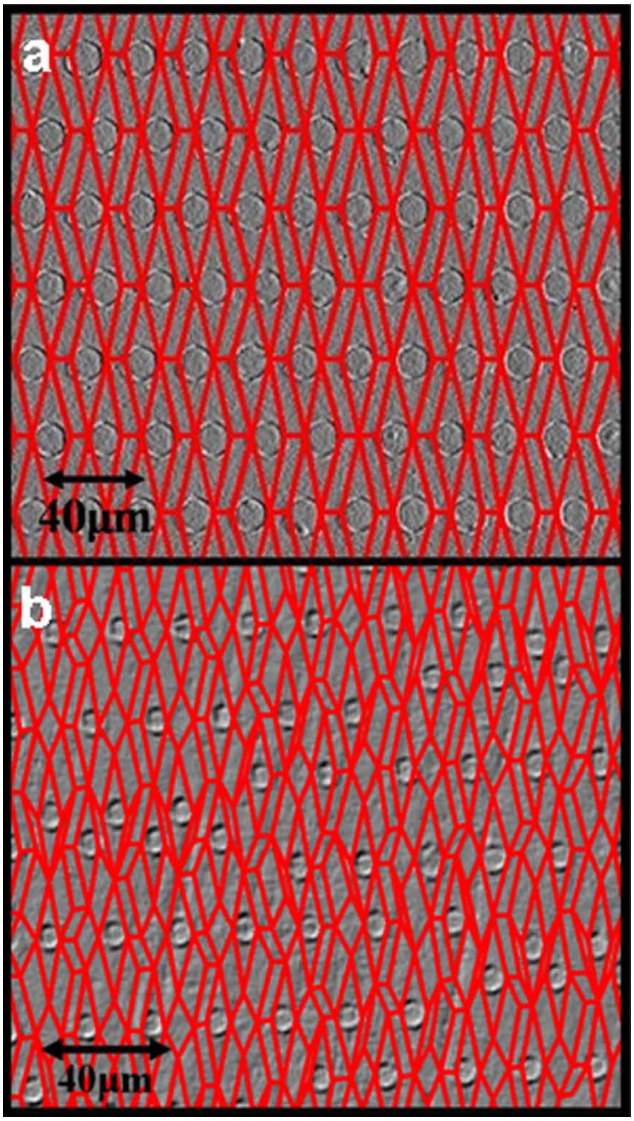

Fig. 1. (Color online) A microscope image of the Z+ surfaces of the NPQCs after selective etching, embedded within the underlying quasi-periodic lattices: (a) the SHG fan, (b) the frequency fan.

within the other parallelograms.

The calculated spectrum of both devices is shown in Fig. 2, embedded within an experimental linear-diffraction picture. The required RLVs are indicated by arrows, validating the utility of the dual-grid method as a discrete-spectrum shaping tool.

The NPQC planar dimensions were 10 mm $\times$6.5 mm, such that the interactions took place along 10 –11 mm (depending on the propagation angle). The calculated magnitudes of the Fourier coefficients are shown in Tables 1 and 2. The conversion efficiency is proportional to the absolute square of the relevant Fourier coefficient [7]. For comparison, the largest coefficient for a one-dimensionally modulated periodic nonlinear photonic crystal used to phase match a single process is $2/\pi \simeq 0.6366$ [7]. These tables also contain the theoretical and experimental results for the efficiency of the processes. Experimentally, a Gaussian pump beam, polarized along the Z axis of the crystal, was focused to a 30 μm waist at

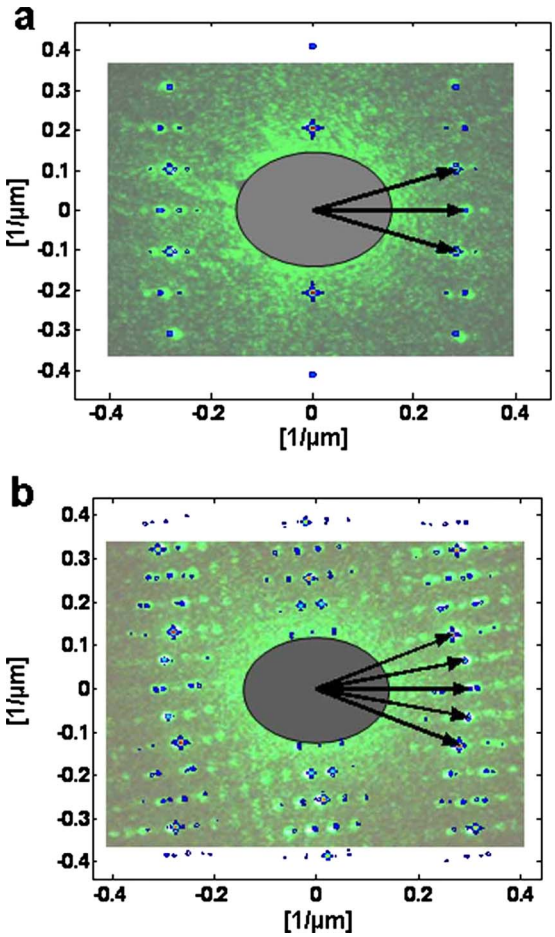

Fig. 2. (Color online) Diffraction picture of the NPQCs. Theoretical calculation embedded within an experimental optical diffraction image. The arrows indicate predefined RLVs. The images went high-pass filtering by removing the diffraction information around the center: (a) the SHG fan, (b) the frequency fan.

the center of the NPQCs. Theoretically, the efficiencies were calculated using the Boyd–Kleinman formalism for interaction of focused Gaussian beams, propagating within a homogeneous nonlinear crystal [16], modified to include the relevant Fourier coefficient. The theoretical +0.5 nm shift of the maximum efficiency is due to calculation of structure parameters under the approximation of plane-wave interaction (all photons with the same exact momentum), which does not take into account the effect of focusing on optimal phase-matching conditions. The experimental +2.5 nm shift is assumed to be due to inaccu-

Table 1. Conversion Efficiencies for the SHG Fan[a]

Propagation Direction [nm]	Fourier Coefficient	Experimental Efficiency [1/W]	Theoretical Efficiency [1/W]
0°	0.1	0.7e–4	1.5e–4
+20°	0.19	1.4e–4	5.2e–4
–20°	0.19	1.2e–4	5.2e–4

[a]The conversion efficiencies in the experiment were measured at 1552 nm. In theory the (maximum) efficiencies were obtained at 1550.5 nm.

Table 2. Conversion Efficiencies for the Frequency Fan[a]

Wavelength [nm]	Fourier Coefficient	Experimental Efficiency [1/W]	Theoretical Efficiency [1/W]
1530	0.1	0.28e−4	1.61e−4
1540	0.05	0.08e−4	0.4e−4
1550	0.035	0.059e−4	0.15e−4
1560	0.05	0.03e−4	0.41e−4
1570	0.1	0.09e−4	1.57e−4

[a]The conversion efficiencies in the experiment were measured at the indicated wavelengths +2.5 nm. In theory the (maximum) efficiencies were obtained at the indicated wavelengths +0.5 nm.

rate dispersion data (Sellmeier equation). The discrepancies in the efficiencies between theory and experiment for the frequency fan are mainly due to imperfections during fabrication; the quasi-periodic pattern was not poled at the same quality all along the NPQC. For the SHG fan the peak efficiencies were given for the indicated propagation directions ±0.5° with FWHM bandwidth of 1.5 nm.

The behavior of the frequency fan device as a function of fundamental wavelength and angle of propagation is shown in Fig. 3. Each parabola represents perfect phase matching under plane-wave conditions given by one of the device-predefined RLVs. The apex of each parabola corresponds to collinear phase matching, whereas the rest of the points corresponds to noncollinear conditions. The experimental results shown in this graph were shifted on the wavelength scale by −2.5 nm. The idealized conditions for collinear phase matching of the entire C band (1530–1570 nm) are shown with a dashed line. The best available path for nearly collinear doubling of the C band is marked with a bold curve. On this path the largest walk-off angle between the input fundamental beam and the output second-harmonic beam is 0.17° (while the largest walk-off for this graph is 0.33°). Thus keeping the propagation direction of the input beam constant and using angle tuning of the NPQC, while staying on this path, allows for nearly collinear doubling of the entire C band.

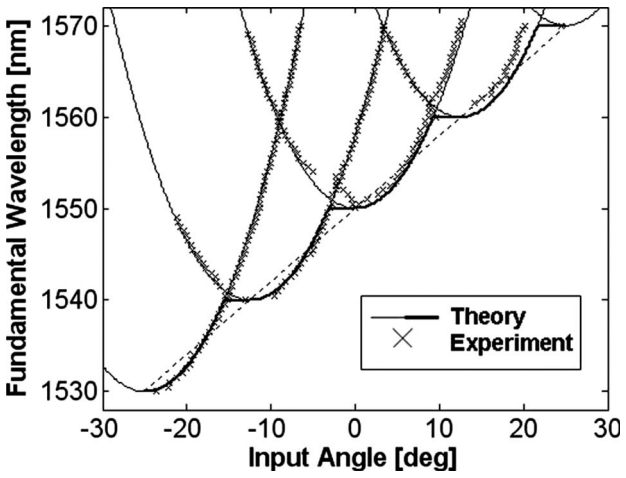

Fig. 3. Phase-matching conditions for the frequency fan as a function of fundamental wavelength and angle of propagation. Each parabola corresponds to one of the predefined RLVs. The dashed line represents idealized collinear phase matching of the C band (1530–1570 nm). In bold is the closest available path to this line. Experimental results were offset by −2.5 nm.

Note that even the simpler SHG fan device functionality can not be reproduced with a periodic 1D structure; to achieve different propagation directions, some combination of angle tuning with wavelength or temperature tuning would be required [17], whereas the SHG fan requires only angle tuning.

We stress that the devices shown in this work are only particular examples, whereas the practical utility of the dual-grid method to phase match any given set of processes is restricted only by limited fabrication resolution, although in principle this restriction can also be circumvented to a degree with higher-order phase matching by using nonprimitive RLVs. The method we use should also be applicable to photonic and phononic crystals while considering lattice-dependent gap formation (Bragg gaps) [18].

This work was partly supported by the Israel Science Foundation, grant 960/05, and by the Israeli Ministry of Science, Culture, and Sport.

References

1. J. A. Armstrong, N. Bloembergen, J. Ducuing, and P. S. Pershan, Phys. Rev. **127**, 1918 (1962).
2. S.-N. Zhu, Y.-Y. Zhu, and N.-B. Ming, Science **278**, 843 (1997).
3. G. I. Stegeman, D. J. Hagan, and L. Torner, Opt. Quantum Electron. **28**, 1691 (1996).
4. V. Berger, Phys. Rev. Lett. **81**, 4136 (1998).
5. N. G. R. Broderick, G. W. Ross, H. L. Offerhaus, D. J. Richardson, and D. C. Hanna, Phys. Rev. Lett. **84**, 4345 (2000).
6. S. Saltiel and Y. S. Kivshar, Opt. Lett. **25**, 1204 (2000).
7. A. Arie, N. Habshoosh, and A. Bahabad, Opt. Quantum Electron. **39**, 361 (2007).
8. K. Fradkin-Kashi, A. Arie, P. Urenski, and G. Rosenman, Phys. Rev. Lett. **88**, 023903 (2001).
9. R. T. Bratfalean, A. C. Peacock, N. G. R. Broderick, K. Gallo, and R. Lewen, Opt. Lett. **30**, 424 (2005).
10. B. Ma, T. Wang, Y. Sheng, P. Ni, Y. Wang, B. Cheng, and D. Zhang, Appl. Phys. Lett. **87**, 251103 (2005).
11. Y. Sheng, J. Dou, B. Cheng, and D. Zhang, Appl. Phys. B **87**, 603 (2007).
12. R. Lifshitz, A. Arie, and A. Bahabad, Phys. Rev. Lett. **95**, 133901 (2005).
13. A. Bahabad, N. Voloch, A. Arie, and R. Lifshitz, J. Opt. Soc. Am. B **24**, 1916 (2007).
14. A. Bahabad, R. Lifshitz, N. Voloch, and A. Arie, Philos. Mag., doi: 10.1080/14786430802060715 (2008).
15. A. Bruner, D. Eger, M. B. Oron, P. Blau, M. Katz, and S. Ruschin, Opt. Lett. **28**, 194 (2003).
16. G. D. Boyd and D. A. Kleinman, J. Appl. Phys. **39**, 3597 (1968).
17. T. Ellenbogen, A. Arie, and S. M. Saltiel, Opt. Lett. **32**, 262 (2007).
18. W. Steurer and D. Sutter-Widmer, J. Phys. D **40**, R229 (2007).